Evaluation of the effect of low soil temperature stress on the land surface energy fluxes simulation in the site and global offline experiments

Siguang Zhu[1, 2], Haishan Chen[1, 2, 3*], Yongjiu Dai[1], Xingjie Lu[1], Wei Shangguan[1], Hua Yuan[1], Nan Wei[1]

1. *KLME/ILCEC/CIC-FMD, Nanjing University of Information Science & Technology (NUIST), Nanjing 210044, China*
2. *School of Atmospheric Sciences, NUIST, Nanjing 210044, China*
3. *NUIST-UoR International Research Institute, NUIST, Nanjing 210044, China*
4. *Southern Marine Science and Engineering Guangdong Laboratory (Zhuhai), Guangdong Province Key Laboratory for Climate Change and Natural Disaster Studies, School of Atmospheric Sciences, Sun Yat-sen University, Guangzhou, Guangdong, China*

Nov 2020

Manuscript submitted to *Journal of Advances in Modeling Earth Systems*

Corresponding author:

Professor **Haishan Chen**

Key Laboratory of Meteorological Disaster, Ministry of Education, Nanjing University of Information Science & Technology, Ningliu Road 219, Nanjing 210044, China

E-mail: haishan@nuist.edu.cn

Information Science & Technology (NUIST), Nanjing, China

E-mail: *haishan@nuist.edu.cn*

Abstract

Low soil temperature stress is a critical factor affecting the root water uptake (RWU) rate of plants. In current land surface models, the RWU amount is determined by the soil water extracted from different soil layers, which calculates by the relative soil water availability and the root fraction of each layer in the rooting zone. The effect of low soil temperature stress is not considered, which may produce biases in the simulation of transpiration. In this study, with the utilization of the in-situ observation data from three FLUXNET sites, we introduced three functions to represent the low soil temperature stress in the Common Land Model (CoLM) and evaluated their effects on the energy fluxes simulation. Then the three low soil temperature stress functions were also evaluated in the global offline simulations by using the FLUXNET-MTE (multi-tree ensemble) data. Results show that the default CoLM overestimates the latent heat flux but underestimates the sensible heat flux in the local spring and early summer at three study sites. By incorporating the low soil temperature stress function into CoLM, the bias in energy flux simulation is significantly reduced. The global offline simulations indicate that considering the effect of low soil temperature stress can improve the model performance on the simulating of the latent heat flux in those high latitude areas. Therefore, we recommend incorporating the effect of low soil temperature stress into land surface models, which is beneficial to increasing the reliability of the models' results, especially over the cold regions.

Keywords: root water uptake; land surface model; low soil temperature stress

Plain Language Summary

Plants obtain water from the soil through their roots, but the process of obtaining water will be affected by a variety of factors. The low temperature in the soil is one of the important influencing factors, which usually reduces the rate of water absorption by plant roots. However, this influence factor is not considered in the current land surface process model. Here, we propose three empirical functions that can represent the effects of low soil temperature, introduce them into the Common Land Model (CoLM), and validate the impact of these functions in the model by using the field observation data. The results of numerical experiments show that considering the effect of low soil temperature on root water uptake in CoLM can improve the simulation performance of the model in many areas.

1. Introduction

How to describe the root water uptake (RWU) process of plants in land surface models is a vital issue (*Feddes et al.*, 2001; *Fu et al.*, 2018). The process of root water uptake is affected by many environmental factors, and the soil temperature is one of them (*Ramos and Kaufmann*, 1979; *Aroca et al.*, 2012). The low soil temperature is serious environmental stress faced by plant roots in the process of RWU (*Kozlowski and Pallardy*, 1997). The low soil temperature usually increases the water flow resistance through the soil-plant-atmosphere continuum direct or indirectly (*Schwarz et al.*, 1997). Even a soil temperature above zero can have a negative effect on the process of RWU (*Murai-Hatano et al.*, 2008). When the atmospheric temperature is high and the soil temperature is still low (for example, in spring), the canopy transpiration demand of plants will be considerable. Restricted by low soil temperature, the RWU rate won't be large enough to supplement the water loss during transpiration, which may cause the detriment of dehydration. When the soil temperature is low, the transport rate of water from the soil to plant roots will decrease and the water viscosity will increase, which leads to less absorption of water through roots (*Running and Reid*, 1980; *Ameglio et al.*, 1990; *Wan et al.*, 2001; *Bloom et al.*, 2004). Besides, the low soil temperature can also inhibit the growth of plant roots, thus reducing the RWU capacity of plants (*Vapaavuori et al.*, 1992; *Zia et al.*, 1994; *Nagasuga et al.*, 2011).

In order to study the effect of low soil temperature stress on the RWU process, many field studies have been carried out by botanists. For example, a study on the response of the RWU rate of cucumber to soil temperature showed that the RWU efficiency of cucumber roots decreases when the soil temperature is below 12 ^{o}C. Above this temperature, the RWU rate doesn't change much (*Satoshi Yoshida and Eguchi*, 1989; *S. Yoshida and Eguchi*, 1991). A field study about rice revealed that the root hydraulic conductivity descends with decreasing soil temperature, and the change in root hydraulic conductivity is most pronounced below 15 ^{o}C (*Murai-Hatano et al.*, 2008). Another field study on the RWU of maize also indicated that the root hydraulic conductivity is proportional to temperature change between 10 ^{o}C and 20 ^{o}C (*Ionenko et al.*, 2010). Reduction of root hydraulic conductivity increases the resistance when soil water enters the root system, which in turn reduces the rate of water uptake by the plant root system. A study on the influence of soil temperature on RWU and transpiration of young Scots pines showed that soil temperature is the main factor behind the decrease of RWU rate of roots under 8 ^{o}C. This study also found that low soil temperature stress can lead to a decrease in stomatal conductance and root activity, which then reduces the root water uptake rate and transpiration (*P. E. Mellander et al.*, 2004). Numerous observational studies have shown that low soil temperature stress is an important factor restricting the soil water supply to plants.

In most of the current land surface models, the RWU rate is calculated by distributing transpiration into each soil layer according to soil water content and root density fraction. Then the water change due to RWU is treated as a sink term and added to the soil vertical water flow equation (*Jarvis*, 1989; *Dickinson et al.*, 1993; *Cox et al.*, 1999; *Dai et al.*, 2003; *Niu et al.*, 2011; *Wang et al.*, 2011; *Yang et al.*, 2011). This parameterization scheme focuses only on the overall water content in the soil and the proportion of plant root density, without considering the influence of various environmental factors including the low soil temperature on the RWU process. With a low soil temperature and a large difference between soil temperature and atmospheric temperature, canopy transpiration will be overestimated by the models accordingly (*P E Mellander et al.*, 2006). Some numerical studies have shown that incorporating the effect of soil temperature into the simulation of RWU can improve the simulation results of the RWU rate and transpiration rate by the models (*Lv et al.*, 2012). Furthermore, improvement of the RWU process in land surface models is beneficial to the prediction of global weather and climate change, carbon and nitrogen cycles and crop yield by earth system models (*Zhu et al.*, 2017).

In this paper, we modified the RWU scheme of the Common Land Model (CoLM) and incorporated three empirical functions to investigate the effect of low soil temperature stress (*Jansson and Karlberg*, 2010). The observation data of three FLUXNET forest sites were used to evaluate the influence of the low soil temperature stress functions on energy flux simulation results. After that, the global offline simulation was carried out to further verify the possible impact of low soil temperature stress functions on the global land surface process simulation. This paper is organized as follows. In section 2, the data sets, model and experimental design are described. Results are presented in the next section, which is followed by the summary and discussions in section 4.

2. Methods

2.1 Model Default

The CoLM is a state-of-the-art land surface model (*Dai et al.*, 2003). It was adopted as the land component for the community atmospheric model (CAM) (*Zeng et al.*, 2002) in the version 2 of the community climate system model (CCSM2) (*Bonan et al.*, 2002) and named as the community land model (CLM). The CoLM has been developed independently in China, and it possesses many new features such as two big leaf models used for leaf temperature and the photosynthesis-stomata resistance, and the two-stream approximation for the calculation of canopy albedo with the solution for singularity point (*Dai et al.*, 2004; *Dai and Ji*, 2005; *Dai et al.*, 2014). As a result, the CoLM is now fundamentally different from both its original version (*Dai et al.*, 2003) and the recent versions of CLM (*Oleson et al.*, 2013; *Lawrence et al.*, 2019). The CoLM has been widely applied to land surface process modeling by many weather forecasting models and climate models.

Low temperature stress in the soil environment can reduce the RWU rate (*Kramer and Boyer*, 1995). In order to account for the effects of low soil temperature stress in the CoLM, a modification of the RWU scheme was conducted in the model. The soil moisture changes in the CoLM were calculated by the following equation:

$$\frac{\partial \theta}{\partial t} = -\frac{\partial q}{\partial z} - E_R \quad (2.1)$$

where θ is the volumetric soil moisture content, t is time (s), z is soil depth (mm), E_R (mm·s^{-1}) is root water extraction and evaporation (only in the surface layer) from the soil, and q is the vertical water flow (mm·s^{-1}).

The sink term $E_{R,j}$ in soil layer *j* was calculated as follows:

$$E_{R,j} = f_{eroot,j} E_{tr} \tag{2.2}$$

where E_{tr} is the transpiration in the canopy (mm·s^{-1}), and $f_{eroot,j}$ refers to the effective root fraction in layer *j*. The effective root fraction $f_{eroot,j}$ that considers both the root fraction and soil water condition was calculated as follows:

$$f_{eroot,j} = \frac{f_{root,j} W_{lt,j}}{\sum f_{root,j} W_{lt,j}} \tag{2.3}$$

where $f_{root,j}$ is the root fraction in soil layer *j*, and $W_{lt,j}$ represents the water stress level in soil layer *j*. In CoLM, the integrated water stress level in all soil layers is represented by f_{roota}, which is the standardization of the sum of $f_{root,j} W_{lt,j}$ in ten soil layers and ranges from 0 to 1. In the default CoLM, the soil temperature is not considered when f_{roota} is calculated. To incorporate the environmental temperature stress into CoLM, the modified f_{roota} was introduced into the RWU scheme:

$$f_{roota,t} = f_t \times f_{roota} \tag{2.4}$$

where $f_{roota,t}$ is the replacement of f_{roota} used for calculating the max canopy potential transpiration $E_{tr,max}$ in the model. The parameter f_t, which represents the effect of low soil temperature stress, varies from 0 to 1. In this study, three different functions originated from the coupled heat and mass transfer model (COUP-MODEL, Jansson and Karlberg, 2010) were used in the CoLM to calculate the value of f_t. The first one is a double-exponential function (*Ågren and Axelsson*, 1980):

$$f_t = 1 - e^{-t_{WA} max(0, Tg - Ttrig)^{t_{WB}}} \tag{2.5}$$

where T_g represents the soil temperature, and T_{trig} is the empirical triggering temperature. When soil temperature gets higher than T_{trig}, the influence of low soil temperature stress decreases gradually. t_{WA} and t_{WB} are the empirical parameters.

The second way to calculate f_t is a polynomial function:

$$f_t = max(0,(\frac{T_g - T_{trig}}{T_{ref} - T_{trig}})^{t_{WE}}) \leq 1 \tag{2.6}$$

where T_{ref} is the reference temperature, and f_t equals 1 when the soil temperature is higher than T_{ref}, which represents the relief of low soil temperature stress when soil temperature is above T_{ref}. And t_{WE} is an empirical parameter.

The third function used to solve the value of f_t is a single-exponential function:

$$f_t = 1 - e^{lg(0.02)\, max(0,\, T_g T_{trig},\, T_{ref} - T_{trig})} \tag{2.7}$$

where the definitions of T_g, T_{trig} and T_{ref} are as same as those in the first two functions. In this study, the values of those parameters in the three functions were set as follows according to the previous work (*P E Mellander et al.*, 2006; *Jansson and Karlberg*, 2010): t_{WA} = -0.0004, t_{WB} = 3, t_{WE} = 2.5, T_{ref} = 16 °C, and T_{trig} = 0°C.

2.2 Data, Sites Description and Experimental Design

FLUXNET is a global network of micrometeorological flux measurement sites that provide long-term ground-based ecosystem observations (*Baldocchi et al.*, 2001). It's very useful for land surface model development (*Friend et al.*, 2007; *Stöckli et al.*, 2008). In this study, we used the observation data from three sites in the FLUXNET 2015 dataset for the investigation (*Pastorello et al.*, 2020). These three sites all have four distinct seasons and plants will encounter low soil temperature stress at the turn of spring and summer. It is suitable to be used for the investigation of the effect of the low soil temperature stress.

The first site is the US-Ha1 site (*Munger*, 1991). This site is located in the forest near Harvard University in Massachusetts, which is in the northeastern US (42.54° N, 72.17° W, 340 meters above sea level, see Figure 1). Since 1989, it has been observing the local sensible heat and latent heat fluxes and the related meteorological variables (*Urbanski et al.*, 2007). The average annual temperature at the location of this site is 6.6 °C, and the average yearly precipitation there is about 1070 mm. The distribution of precipitation is relatively uniform throughout the year (Figure 2). Vegetation around the site is dominated by *Quercus rubra* and *Acer rubrum*, and sporadic distribution of eastern *Tsuga canadensis*, *Pinus strobus*, and *Pinus resinosa* can also be found. The observation height of this site is 30 m. The observation data period used in this study is from 1994 to 2001. The International Geosphere-Biosphere Programme (IGBP) type is Deciduous Broadleaf Forests (DBF).

The second site is the FI-Let site (*Koskinen et al.*, 2014), which is located at Lettosuo in southern Finland (60.64 ° N, 23.96 ° E, 111 meters above sea level, Figure 1). The average annual temperature at this site is about 4.5 °C, and the annual mean precipitation is about 548 mm (Figure 2). The dominating species around the site is Scots pine (Pinus sylvestris), Norway spruce (*Picea abies*), and birch (*Betula pubescens*). Other species are also common there like *Dryopteris carthusiana* and *Vaccinium myrtillus*. The observation height of this site is 25.5 m. The observation data period used in this study is from 2010 to 2011. The IGBP type is Evergreen Needleleaf Forests (ENF) and almost all trees remain green all year.

The third site is the FI-Hyy site (*Suni et al.*, 2003), a forest site locate at Hyytiälä in central Finland next to Lake Kuivajärvi (61.85 ^{o} N, 24.29 ^{o} E, meters above sea level, as shown in Figure 1). This site has short summers, cold winters, and relatively low annual precipitation (the annual mean temperature is about 4.3 °C, and the annual mean precipitation is about 604 mm, see Figure 2). The dominating species at this site is Scots pine (*Pinus sylvestris*), The observation height is 23.3 m. The observation data period used in this study is from 2009 to 2013. The IGBP type for this site is also ENF.

With the observation data from these three sites, four sets of different numerical experiments were designed to study the effects of the three low soil temperature stress functions on the model results. The experimental design is shown in Table 1. The atmospheric driving data required for the experiments were all from the observations datasets at the three sites. The time resolution was once every half an hour. Each set of simulations was run for 30 years by looping the driving data, with spin-up employed to balance the initial model variables. The soil physical parameters used in the experiments were all derived from the soil data set of the CoLM model(*Shangguan et al.*, 2014). The LAI data used in the study are from the LAI dataset developed by members of the CoLM team based on the MODIS satellite inversion data. (*Yuan et al.*, 2011)

To evaluate the effect of the low soil temperature stress in middle and high latitudes, we also preliminarily investigated it in the global offline simulation. Four global offline simulations designed like the single point experiments (S01, S02, S03, and S04) were conducted to evaluate the global performance of CoLM with the three low soil temperature stress functions. These global simulations were run from 1985 to 2004, driven by the forcing data from the National Center for Atmospheric Research (*Qian et al.,* 2006). The first ten years were used as spin-up and the last ten years were used for analysis. The spatial resolution was T62 (192 longitude grid points and 94 latitude grid points). Then we used the FLUXNET-MTE (multi-tree ensemble) global land latent heat flux product (*Jung et al.*, 2009) to evaluate the model's performance with the default and revised RWU schemes.

2.3 Statistical Analysis

To evaluate the performance of the default and modified RWU schemes in CoLM, the root mean square error (RMSE) and the agreement index d (*Willmott*, 1981) between the observed data and simulated results were employed. They were calculated as follows respectively:

$$RMSE = \sqrt{\frac{\sum_{i=1}^{n}\left(P_i - O_i\right)^2}{n-1}} \qquad (2.8)$$

$$d = 1 - \frac{\sum_{i=1}^{n}\left(P_i - O_i\right)^2}{\sum_{i=1}^{n}\left(\left|P_i - \bar{O}\right| + \left|O_i - \bar{O}\right|\right)^2} \qquad (2.9)$$

In these two functions, P_i and O_i are the simulated and observed fluxes at time step *i* in the CoLM. $\bar{O}$ refers to the average of the observed fluxes, and *n* is the total number of observed data. The observed fluxes used in this study are half-hourly, and they were used in the native time sampling. The value of RMSE is always greater than 0, and the closer it is to 0, the closer the simulation result is to the observation. Index d varies from 0 to 1, and a value of 1 indicates a perfect match between the simulation and observation, while 0 implies no agreement at all.

3. Results

When plants are exposed to low temperature stress in the soil environment, the water uptake rate of the root system will decrease under the influence of low temperature. A low temperature in the soil environment will reduce the root water conductivity, increase the viscosity of water in the soil, and inhibit the growth of the plants' root system, which will lead to a decrease in the RWU rate of the plants. In the most up-to-date land surface models, the parameterization scheme of the RWU process cannot show the effect of low soil temperature stress. In order to improve the RWU parameterization scheme in the land surface model and evaluate the effect of low soil temperature stress on the simulation of land surface processes, in this study we incorporated a modified RWU scheme into the CoLM model with three different functions representing the effect of low soil temperature stress. The in-situ data from three FLUXNTE sites were used in this study to validate the performance of the modified model. The temperature differences between the soil and air are quite large at these sites in the local spring and early summer, creating an ideal condition for studying the impact of low soil temperature stress on the RWU process (Figure 3).

In this study, we compared the simulation results of the sensible heat flux (Qh) and latent heat flux (Qle) in the control run (S01) and three experimental runs (S02, S03, and S04, the definitions are in Table 1). Figure 4 illustrates the comparison between the observed and simulated mean diurnal fluxes of Qh and Qle at the US-Ha1 site. It can be found from the figure that in the local spring and early summer (March, April, and May, MAM), compared with the observed data, the model results significantly underestimate the daytime sensible heat flux, especially at noon. After considering the effect of low temperature stress in soil on the RWU process in CoLM, the Qh simulation results from the three sensitivity experiments are improved, and the simulated values of daytime Qh are closer to the observation (Figure 4a). Regarding the simulation of Qle, the daytime Qle is significantly overestimated in the control experiment (S01), which is revised in the three sensitivity simulations (S02, S03, and S04) after introducing low soil temperature stress into the RWU process. Among the three sensitivity experiments, S02 (the double-exponential function) and S03 (the polynomial function) produce almost the same simulation results of Qle, while the Qle results of S04 (the single-exponential function) are relatively closer to the observed Qle values (Figures 4a and 4b). According to a comparison between the observed and simulated average annual diurnal Qh, the control run (S01) underestimates the daytime Qh (Figures 4c and 4d). However, the differences between the simulated and observed values are smaller than those in spring. Results for Qh from the three sensitivity runs are relatively closer to the observed values. The Qh results of S02 and S03 are almost the same and closer to the observed data at noon. The comparison between the observed and simulated annual mean diurnal Qle suggests that an overestimation of the daytime Qle still exists in the control run. After the inclusion of the effect of low soil temperature stress in the three sensitivity experiments, the simulated Qle decreases significantly in the daytime (Figures 4c and

4d). The results of S02 and S03 are almost the same, and S04 yields values that are much closer to the observed Qle than the other sensitivity runs. At the FI-Let site and the FI-Hyy site, the differences in Qh and Qle between the observation data and four experimental simulations were relatively smaller than that of the US-Ha1 site (Figures 5 and 6). In the local spring and early summer (May, June, and July, MJJ), the control run greatly underestimated the daytime Qh and overestimated the daytime Qle at these two sites. After considering low soil temperature stress in the model, the simulation results of Qh and Qle in MJJ are greatly improved, which is quite consistent with the observation data (Figures 5a, 5b, 6a, and 6b). Bothe the Qh and Qle results of the three experimental runs are relatively close to each other, among which the results of S04 are rather better. In the annual average results, the deviation of the control run in simulating Qh and Qle is smaller than that in MJJ at these two sites. The model performance for reproducing the variations of half-hour Qh and Qle is also improved after considering the effect of low soil temperature stress at the FI-Let site and the FI-Hyy site (Figures 5c, 5d, 6c, and 6d). These findings indicate that inclusion of the effect of low soil temperature stress on the RWU process can be beneficial to counteracting the overestimation of Qle by CoLM in regions with considerable air-soil temperature differences during the local spring and early summer.

When reproducing the seasonal variation of the climatically averaged energy fluxes at three FLUXNET sites, the modified RWU scheme mainly affects simulation results of the energy fluxes in the local spring and early summer. As can be seen from Figure 7, the control run indicates that the CoLM can well simulate the seasonal variation of Qh and Qle. However, in the results of the control run, the simulated Qh is lower than the observed values in the local spring and early summer at three FLUXNET sites. The underestimation of Qh in the control run during local spring and early summer at the US-Ha1 site is particularly obvious (Figure 7a), while at the FI-Let site and the FI-Hyy site, the underestimation degree of Qh in the control run is relatively smaller (Figures 7c and 7e). By taking the effect of low soil temperature stress into consideration, the three experimental simulations correct the underestimation of Qh in the default model. Especially at the US-Ha1 site, after considering the low soil temperature stress, the value of Qh in the simulation results increased the most (Figure 7a). At the US-Ha1 site, similar results are gained by experiments S02 and S03, which are closer to the observed Qh in May, while in June and July, the Qh simulated by S02 and S03 is relatively higher than the observed values. The Qh given by S04 is slightly lower than that in S02 and S03 in May, while in June and July, the Qh in S04 is much closer to the observed values. In terms of Qle, the differences between the three experimental runs and the control run are also primarily concentrated in the local spring and summer. The control experiment S01 significantly overestimates the Qle values in the local spring and early summer, while the experimental runs S02 and S03 underestimate the Qle in midsummer. In comparison, the simulation result of Qle by S04 is the closest to the observation. At the FI-Let site, the differences of Qh and Qle between the three experimental runs and control run was relatively smaller, mainly in May, June, and July (Figures 7c and 7d). For the simulation of Qle, S04 performed fairly better than the other two experiments. At the

FI-Hyy site, in May and June, the Qh results of S04 are relatively closer to the observation data than those of the other two sites. As to reproduce the Qle, S02 and S03 are relatively closer to the observation data than S04 during May and June. However, the S02 and S03 slightly overestimate the Qle and S04 performed a little better than them in July (Figures 7e and 7f). This further indicates that incorporating the low soil temperature stress might help improve the capability of CoLM to simulate the surface energy fluxes in spring and summer at this site, and yet has limited effect in autumn and winter.

Figure 8 shows the simulation results of the interannual variation of the energy fluxes by the control run and three experimental runs. For the simulation of the interannual variation of Qle (Qh), the control experiment can reproduce the interannual variation curve to a certain extent at three FLUXNET sites, however, an overestimation (underestimation) can be found in local spring and early summer for almost every year in the control run (Figure 8). The results of the three experimental runs indicate that this overestimation (underestimation) of Qle (Qh) can be corrected by including low soil temperature stress in the parameterization scheme of the RWU process. At the US-Ha1 site, in the experiments S02 and S03, the simulation results underestimate the summer Qle in some years, while in S04, this deviation is not so obvious (Figures 8a and 8b). At the FI-Let site, the three experimental runs performed relatively similar and got much closer to the observation data than the control run in each study year (Figures 8c and 8d). As to the FI-Hyy site, the experiments S02 and S03 still lead to nearly the same results. These two runs simulated Qh relatively better than S04 in some years. In the Qle results, the S04 run performed better in reproducing Qle during the local spring and early summer (Figures 8e and 8f). The above analysis suggests that among the three low soil temperature stress functions, the single-exponential function (S04) is relatively more suitable for improving the energy flux simulation by CoLM than the other two functions.

From the scatter diagram of the observed and simulated daily energy fluxes at the US-Ha1 site, it can also be found that the slope of the linear regression trend line between the Qh simulation results of the control experiment (S01) and the observed Qh values is much less than 1 (Figure 9). It indicates that the Qh simulated by the default CoLM is lower than the in-situ data. In the three sensitivity runs, the slope of the linear regression trend line is closer to 1, which means the deviation from the observed Qh in S01 is corrected to some extent (Figures 9a, 9b, 9c, and 9d). For Qle, the result from S01 is relatively higher than observations, and the slope of the linear regression trend line is greater than 1. However, the Qle simulated by S02 and S03 has lower values than the observed Qle, which corresponds to the linear regression trend lines with slopes below 1. The Qle simulation result by S04 is closer to the observations, and the slope of its linear regression trend line is the closest to 1 among the three sensitivity runs (Figures 9e, 9f, 9g, and 9h).

By comparing the statistical index RMSE and the agreement index b, we can further quantitatively evaluate how the energy flux simulation is improved by incorporating the effect of low soil temperature stress. As shown in Table 2, at the US-Ha1 site, during the local spring and early summer, the agreement index of Qh and Qle results in the three experimental runs is higher than that of the control experiment, while the RMSE is about 20% lower than that of the latter. The three experimental runs slightly differ in terms of simulation performance, and S03 performs a little bit better in spring according to the statistical comparison. For the annual mean results of Qh and Qle, all three sensitivity runs also generate better performance than the control run. Among the four simulations, S04 yields the highest b values and the lowest RMSE values for both Qh and Qle, indicating that the S04 run has the best performance on reproducing energy fluxes at this site. At the FI-Let site, a similar conclusion as the US-Ha1 site can be drawn. Although the differences in the RMSE and agreement index between the control run and three experimental runs are relatively small. At the FI-Hyy site, in the local spring and early summer (MJJ), the RMSE values for Qh and Qle in the results of S02, S03, and S04 decreased by as much as 30% compared to the control run. And the agreement index values increased about 0.1 in the three experiments considering the low soil temperature stress in MJJ. In the annual results, the degree of improvement in the statistical indexes in the three experimental runs is significantly reduced, which is similar to the other two sites. The comparison indicates that by introducing the effect of low soil temperature stress into the RWU process, the revised CoLM can improve its capability for simulating the energy fluxes.

CoLM is a land surface model, which is designed for providing the boundary condition to the climate model. Therefore, it is necessary to verify what role these low soil temperature stress functions will have if they are used in global scale simulation and whether they will make the model results more unstable. To this end，we also conducted four groups of global offline experiments like the single point experiments (S01, S02, S03, and S04, see Table 1) to investigate the effect of low temperature soil stress on global latent heat flux simulation in CoLM. The simulation results suggest that the low soil temperature stress functions have almost no effect in tropical and subtropical regions. The default CoLM overestimation the Qle in many areas over middle and high latitudes in the boreal spring and summer (Figures 10a and 10b). Considering the low soil temperature stress in the model will reduce the overestimation of Qle in the model results, thus making the results closer to the FLUXNET-MTE data (Figures 10c-10h). However, during autumn and winter in the Northern Hemisphere, three low soil temperature stress functions have little effect on the simulation results of Qle (Figure 11). On the global scale, there is little difference in the simulation performance of the three low temperature stress functions. Concerning the regional results, in North America, the three low soil temperature stress functions help to reduce the overestimation of Qle in spring. In Siberia, from May to September, by introducing the low temperature soil stress, the Qle simulation results are improved and the overestimation of Qle in the simulation by S01 is reduced (Figure 12). The above findings show that the overestimation of Qle in the default CoLM could be reduced by further including the low temperature soil stress effect in many areas over middle and high latitudes such as North America, North Europe, and Siberia. While for other regions, this inclusion won't affect the effect of the original RWU scheme on the simulation.

4. Summary and Discussion

The process of plant water uptake is affected and regulated by various factors, among which the low soil temperature stress is a vital one. Low soil temperature can reduce the activity of root cells, increase the viscosity coefficient of soil water, and reduce the water absorption rate of plant roots. In spring and early summer, there is a large gap between soil and atmospheric temperature, which can reduce the rate of RWU and transpiration of plants, hinder the dehydration, and affect the growth of plants. In most of the current land surface models, the parameterization scheme of the RWU process is relatively simple, and the effect of low soil temperature stress on the RWU process is not taken into account, especially when the difference between the soil and air temperature is considerable. In this study, we modified the RWU scheme of CoLM by introducing three empirical functions to represent the effect of low soil temperature stress (*Jansson and Karlberg*, 2010), and evaluated the impact of low soil temperature stress on the energy flux simulation results in three forest sites.

In this paper, we selected three FLUXNET sites (US-Ha1, FI-Let, and FI-Hyy) with noticeable seasonal variation as the research sites, and used local observation data to evaluate the effect of low soil temperature stress on the simulation of land surface energy fluxes by CoLM. The results show that the default CoLM has a certain capability to simulate the variations of Qh and Qle on different time scales at the three FLUXNET sites. However, the control experiment suggests that without considering the effect of low soil temperature stress, the RWU parameterization scheme in the default CoLM can lead to an underestimation of the daytime Qh and an overestimation of the daytime Qle. According to the average annual results, this underestimation of Qh and overestimation of Qle mainly occur in the local spring and early summer. The inclusion of low soil temperature stress is beneficial to correct the underestimation of Qh and overestimation of Qle in the local spring and early summer and can improve the capability of CoLM to simulate the diurnal and seasonal variations of the land surface energy fluxes at these study sites. The three low soil temperature stress functions adopted in this study can all improve the simulation results of energy fluxes. Whether in the simulation of Qh and Qle, the results of S02 (the double-exponential function) and S03 (the polynomial function) are almost the same, which indicates that despite the different forms of these two functions, their effects on the simulation results are very similar. This may be due to the empirical choice of parameters in these two functions, as particular combinations of parameters can make different forms of functions have similar effects. On the other side, the Qh and Qle results of S04 (the single-exponential function) are fairly better, and the underestimation of midsummer Qle found in S02 and S03 doesn't occur in the results of S04. This function and the parameters in it are more suitable for improving the model performance at these three forest sites. In the global offline simulations, the three low soil temperature stress functions were also added to CoLM. Consequently, the model simulates the latent heat in North America, North Europe, and Siberia better, the overestimation of Qle at these regions was revised.

Low soil temperature stress is widespread in non-tropical areas around the world, and its impact on the RWU process cannot be ignored. Improving the parameterization scheme of the RWU process in land surface models by taking the effect of low soil temperature stress into consideration helps to improve the simulation skill of the RWU, canopy transpiration, and energy fluxes of the land surface in land surface models. The land surface models are also a part of the earth system models, and thus their improvement can contribute to enhanced confidence in the simulation of global climate change. This study demonstrates that the low soil temperature stress can significantly impact the simulation of the surface energy fluxes, which is worthy of more detailed research and evaluation in future work.

The uncertainty caused by various parameterization schemes in land surface models is pervasive in the simulation of land surface processes. In this study, the parameters of several low soil temperature stress functions are obtained empirically based on some observed data, which brings some uncertainty to the evaluation of the model results. However, the results of this paper also show that these empirical parameters are effective for characterizing the effects of low soil temperature stress in the land surface model. When this set of parameters is applied to the global simulation, it also has a good applicability between different vegetation types. This may be due to the fact that low soil temperature stress mainly occurs in middle and high latitudes, which limits the areas and vegetation types (mainly ENF and DBF) where low soil temperature stress functions may play a role. In future work, it is necessary to further optimize these empirical parameters, but this requires a large number of field observation data and a large number of model simulation testing work, because the observation of plant physiology and ecology is more difficult, and the representativeness of field observation data is also limited. However, with the amounts of satellite remote sensing data and field observation data increasing, more data can be used for the evaluation and optimization of land surface parameterization schemes. Based on further evaluation and optimization, the function of low soil temperature stress can be more accurate, and the parameters used can better reflect the characteristics of local vegetation.

Acknowledgments

This work was supported by the Natural Science Foundation of China (grants 41905075). The FLUXNET 2015 datasets are available at https://fluxnet.org/. The authors thank J. W. Munger, the PI of the US-Ha1 site, Barbara Godzik, Timo Vesala, Eero Nikinmaa, and Janne Levula, the PIs of the FI-Hyy site, Annalea Lohila, Mika Korkiakoski, and Tuomas Laurila, the PIs of the FI-Let site for providing the data openly. The code and the datasets of the CoLM can be downloaded from http://globalchange.bnu.edu.cn/research/. The forcing data for the global offline simulations can be achieved at https://svn-ccsm-inputdata.cgd.ucar.edu/trunk/inputdata. The authors would like to express gratitude to the related researchers and institutes for providing the data.

References

Ågren, G. I., and B. Axelsson (1980), PT: A Tree Growth Model, *Ecological*

Bulletins(32), 525-536.

Ameglio, T., J. Morizet, P. Cruiziat, M. Martignac, C. Bodet, and H. Raynaud (1990), The effects of root temperature on water flux, potential and root resistance in sunflower, *Agronomie (Paris)*, doi: 10.1051/agro:19900407.

Aroca, R., R. Porcel, and J. M. Ruiz-Lozano (2012), Regulation of root water uptake under abiotic stress conditions, *Journal of Experimental Botany*, 63(1), 43-57, doi: 10.1093/jxb/err266.

Baldocchi, D., E. Falge, L. Gu, R. Olson, D. Hollinger, S. Running, et al. (2001), FLUXNET: A New Tool to Study the Temporal and Spatial Variability of Ecosystem-Scale Carbon Dioxide, Water Vapor, and Energy Flux Densities, *Bulletin of the American Meteorological Society*, 82(7046), 2415-2434, doi: 10.1175/1520-0477(2001)082<2415:FANTTS>2.3.CO;2.

Bloom, A. J., M. A. Zwieniecki, J. B. Passioura, L. B. Randall, N. M. Holbrook, and D. A. St. Clair (2004), Water relations under root chilling in a sensitive and tolerant tomato species, *Plant, Cell and Environment*, 27(8), 971-979, doi: 10.1111/j.1365-3040.2004.01200.x.

Bonan, G. B., K. W. Oleson, M. Vertenstein, S. Levis, X. Zeng, Y. Dai, et al. (2002), The land surface climatology of the community land model coupled to the NCAR community climate model, *Journal of Climate*, 15(22), 3123-3149, doi: 10.1175/1520-0442(2002)015<3123:TLSCOT>2.0.CO;2.

Cox, P. M., R. A. Betts, C. B. Bunton, R. L. H. Essery, P. R. Rowntree, and J. Smith (1999), The impact of new land surface physics on the GCM simulation of climate and climate sensitivity, *Climate Dynamics*, 15(3), 183-203, doi: 10.1007/s003820050276.

Dai, Y., and D. Ji (2005), The Common Land Model (CoLM) User's Guide, edited.

Dai, Y., R. E. Dickinson, and Y.-P. Wang (2004), A two-big-leaf model for canopy temperature, photosynthesis, and stomatal conductance, *Journal of Climate*, 17(12), 2281-2299, doi: 10.1175/1520-0442(2004)017<2281:ATMFCT>2.0.CO;2.

Dai, Y., W. Shangguan, H. Yuan, S. Zhang, S. Zhu, and X. Zhang (2014), The Common Land Model (CoLM) Version 2014, edited by Y. Dai, http://globalchange.bnu.edu.cn/research/models.

Dai, Y., X. Zeng, R. E. Dickinson, I. Baker, G. B. Bonan, M. G. Bosilovich, et al. (2003), The common land model, *Bulletin of the American Meteorological Society*, 84(8), 1013-1023, doi: 10.1175/BAMS-84-8-1013.

Dickinson, R. E., a. Henderson-Sellers, and P. J. Kennedy (1993), Biosphere-Atmosphere ransfer Scheme (BATS) version 1e as coupled to the NCAR Community Climate Model, *Journal of Geophysical Research*, TN387+STR(D2), 72 pp, doi: 10.1029/2009JD012049.

Feddes, R. A., H. Hoff, M. Bruen, T. Dawson, P. de Rosnay, P. Dirmeyer, et al. (2001), Modeling root water uptake in hydrological and climate models, *Bulletin of the American Meteorological Society*, 82(12), 2797-2809, doi: 10.1175/1520-0477(2001)082<2797:MRWUIH>2.3.CO;2.

Friend, A. D., A. Arneth, N. Y. Kiang, M. Lomas, J. Ogee, C. RÖDENBECK, et al.

(2007), FLUXNET and modelling the global carbon cycle, *Global Change Biology*, 13(3), 610-633, doi: 10.1111/j.1365-2486.2006.01223.x.

Fu, C., G. Wang, K. Bible, M. L. Goulden, S. R. Saleska, R. L. Scott, et al. (2018), Hydraulic redistribution affects modeled carbon cycling via soil microbial activity and suppressed fire, *Global Change Biology*, 24(8), 3472-3485, doi: 10.1111/gcb.14164.

Ionenko, I. F., A. V. Anisimov, and N. R. Dautova (2010), Effect of temperature on water transport through aquaporins, *Biologia Plantarum*, 54(3), 488-494, doi: 10.1007/s10535-010-0086-z.

Jansson, P., and L. Karlberg (2010), Coupled heat and mass transfer model for soil-plant-atmosphere systems. Royal Institute of Technology, Stockholm, 484 pp, edited.

Jarvis, N. (1989), A simple empirical model of root water uptake, *Journal of Hydrology*, 107(1), 57-72, doi: 10.1016/0022-1694(89)90050-4.

Jung, M., M. Reichstein, and A. Bondeau (2009), Towards global empirical upscaling of FLUXNET eddy covariance observations: validation of a model tree ensemble approach using a biosphere model, *Biogeosciences*, 6(10), 2001-2013, doi: 10.5194/bg-6-2001-2009.

Koskinen, M., K. Minkkinen, P. Ojanen, M. Kämäräinen, T. Laurila, and A. Lohila (2014), Measurements of CO₂ exchange with an automated chamber system throughout the year: challenges in measuring night-time respiration on porous peat soil, *Biogeosciences*, 11(2), 347-363, doi:

10.5194/bg-11-347-2014.

Kozlowski, T., and S. Pallardy (1997), Growth control in woody plants, *Academic Press*.

Kramer, P. J., and J. S. Boyer (1995), Water relations of plants and soils, *Academic press*.

Lawrence, D. M., R. A. Fisher, C. D. Koven, K. W. Oleson, S. C. Swenson, G. Bonan, et al. (2019), The Community Land Model Version 5: Description of New Features, Benchmarking, and Impact of Forcing Uncertainty, *Journal of Advances in Modeling Earth Systems*, 11(12), 4245-4287, doi: 10.1029/2018ms001583.

Lv, G., W. Hu, Y. Kang, B. Liu, L. Li, and J. Song (2012), Root Water Uptake Model Considering Soil Temperature, *Journal of Hydrologic Engineering*, 18(4), 441, doi: 10.1061/(ASCE)HE.1943-5584.0000642.

Mellander, P. E., K. Bishop, and T. Lundmark (2004), The influence of soil temperature on transpiration: a plot scale manipulation in a young Scots pine stand, *Forest Ecology and Management*, 195(1-2), 15-28, doi: 10.1016/j.foreco.2004.02.051.

Mellander, P. E., M. Stahli, D. Gustafsson, and K. Bishop (2006), Modelling the effect of low soil temperatures on transpiration by Scots pine, *Hydrological Processes*, 20(9), 1929-1944, doi: 10.1002/hyp.6045.

Munger, J. W. (1991), (1991-) AmeriFlux US-Ha1 Harvard Forest EMS Tower (HFR1), *Dataset.*, doi: 10.17190/AMF/1246059.

Murai-Hatano, M., T. Kuwagata, J. Sakurai, H. Nonami, A. Ahamed, K. Nagasuga, et al. (2008), Effect of Low Root Temperature on Hydraulic Conductivity of Rice Plants and the Possible Role of Aquaporins, *Plant and Cell Physiology*, 49(9), 1294-1305, doi: 10.1093/pcp/pcn104.

Nagasuga, K., M. Murai-Hatano, and T. Kuwagata (2011), Effects of Low Root Temperature on Dry Matter Production and Root Water Uptake in Rice Plants, *Plant Production Science*, 14(1), 22-29, doi: 10.1626/pps.14.22.

Niu, G.-Y., Z.-L. Yang, K. E. Mitchell, F. Chen, M. B. Ek, M. Barlage, et al. (2011), The community Noah land surface model with multiparameterization options (Noah-MP): 1. Model description and evaluation with local-scale measurements, *Journal of Geophysical Research: Atmospheres*, 116(D12), doi: 10.1029/2010jd015139.

Oleson, K., D. Lawrence, G. Bonan, B. Drewniak, M. Huang, C. Koven, et al. (2013), Technical description of version 4.5 of the Community Land Model (CLM). NCAR Tech*Rep.*, Note NCAR/TN-503+ STR. National Center for Atmospheric Research, Boulder, CO, 422 pp. doi: 10.5065/D6RR1W7M.

Pastorello, G., C. Trotta, E. Canfora, H. Chu, D. Christianson, Y.-W. Cheah, et al. (2020), The FLUXNET2015 dataset and the ONEFlux processing pipeline for eddy covariance data, *Scientific Data*, 7(1), 225, doi: 10.1038/s41597-020-0534-3.

Qian, T., A. Dai, K. E. Trenberth, and K. W. Oleson (2006), Simulation of global land surface conditions from 1948 to 2004. Part I: Forcing data and evaluations, *Journal of Hydrometeorology*, 7(5), 953-975, doi: 10.1175/Jhm540.1.

Ramos, C., and M. R. Kaufmann (1979), Hydraulic Resistance of Rough Lemon Roots, *Physiologia Plantarum*, 45(3), 311-314, doi: 10.1111/j.1399-3054.1979.tb02589.x.

Running, S. W., and C. P. Reid (1980), Soil Temperature Influences on Root Resistance of Pinus contorta Seedlings, *Plant Physiology*, 65(4), 635-640, doi: 10.1104/pp.65.4.635.

Schwarz, P. A., T. J. Fahey, and T. E. Dawson (1997), Seasonal air and soil temperature effects on photosynthesis in red spruce (Picea rubens) saplings, *Tree Physiology*, 17(3), 187-194, doi: 10.1093/treephys/17.3.187.

Shangguan, W., Y. Dai, Q. Duan, B. Liu, and H. Yuan (2014), A global soil data set for earth system modeling, *Journal of Advances in Modeling Earth Systems*, 6(1), 249-263, doi: 10.1002/2013ms000293.

Stöckli, R., D. Lawrence, G. Y. Niu, K. Oleson, P. Thornton, Z. L. Yang, et al. (2008), Use of FLUXNET in the Community Land Model development, *Journal of Geophysical Research: Biogeosciences*, 113(G1), doi: 10.1029/2007JG000562.

Suni, T., J. Rinne, A. Reissell, N. Altimir, P. Keronen, U. Rannik, et al. (2003), Long-term measurements of surface fluxes above a Scots pine forest in Hyytiala, southern Finland, 1996-2001, *Boreal Environment Research*, 8(4), 287-302.

Urbanski, S., C. Barford, S. Wofsy, C. Kucharik, E. Pyle, J. Budney, et al. (2007), Factors controlling CO2 exchange on timescales from hourly to decadal at Harvard Forest, *Journal of Geophysical Research: Biogeosciences*, 112(G2), doi:

10.1029/2006jg000293.

Vapaavuori, E. M., R. Rikala, and A. Ryyppö (1992), Effects of root temperature on growth and photosynthesis in conifer seedlings during shoot elongation, *Tree Physiology*, 10(3), 217-230, doi: 10.1093/treephys/10.3.217.

Wan, X., J. J. Zwiazek, V. J. Lieffers, and S. M. Landhäusser (2001), Hydraulic conductance in aspen (Populus tremuloides) seedlings exposed to low root temperatures., *Tree Physiology*, 21(10), 691-696, doi: 10.1093/treephys/21.10.691.

Wang, Y. P., E. Kowalczyk, R. Leuning, G. Abramowitz, M. R. Raupach, B. Pak, et al. (2011), Diagnosing errors in a land surface model (CABLE) in the time and frequency domains, *Journal of Geophysical Research: Biogeosciences*, 116, 1-18, doi: 10.1029/2010JG001385.

Willmott, C. J. (1981), On the validation of models, *Physical geography*, 2(2), 184-194, doi: 10.1080/02723646.1981.10642213.

Yang, Z.-L., G.-Y. Niu, K. E. Mitchell, F. Chen, M. B. Ek, M. Barlage, et al. (2011), The community Noah land surface model with multiparameterization options (Noah-MP): 2. Evaluation over global river basins, *Journal of Geophysical Research: Atmospheres*, 116(D12), doi: 10.1029/2010jd015140.

Yoshida, S., and H. Eguchi (1989), Effect of root temperature on gas exchange and water uptake in intact roots of cucumber plants (Cucumis sativus L.) in hydroponics, *Biotronics*, 18, 15-21.

Yoshida, S., and H. Eguchi (1991), Root temperature effect on hydraulic characteristics of roots in hydroponics, *IFAC Proceedings Volumes*, 24(11), 153-158, doi: 10.1016/B978-0-08-041273-3.50032-X.

Yuan, H., Y. Dai, Z. Xiao, D. Ji, and W. Shangguan (2011), Reprocessing the MODIS Leaf Area Index products for land surface and climate modelling, *Remote Sensing of Environment*, 115(5), 1171-1187, doi: doi.org/10.1016/j.rse.2011.01.001.

Zeng, X., M. Shajkh, Y. Dai, R. E. Dickinson, and R. Myneni (2002), Coupling of the Common Land Model to the NCAR Community Climate Model, *Journal of Climate*, 15(14), 1832-1854, doi: 10.1175/1520-0442(2002)015<1832:COTCLM>2.0.CO;2.

Zhu, S., H. Chen, X. Zhang, N. Wei, W. Shangguan, H. Yuan, et al. (2017), Incorporating root hydraulic redistribution and compensatory water uptake in the Common Land Model: Effects on site level and global land modeling, *Journal of Geophysical Research: Atmospheres*, 122(14), 7308-7322, doi: 10.1002/2016jd025744.

Zia, M. S., M. Salim, M. Aslam, M. A. Gill, and Rahmatullah (1994), Effect of Low Temperature of Irrigation Water on Rice Growth and Nutrient Uptake, *Journal of Agronomy and Crop Science*, 173(1), 22-31, doi: 10.1111/j.1439-037X.1994.tb00570.x.

Figure Captions:

Figure 1. The location and the IGBP (International Geosphere-Biosphere Programme) type of the US-Ha1 site, the FI-Let site, and the FI-Hyy site.

Figure 2. Observed climatological monthly averaged precipitation (bar) and temperature (line with the circle) at the US-Ha1 site (top), the FI-Let site (middle), and the FI-Hyy site (bottom).

Figure 3. Simulated climatological daily averaged of air temperature (blue line, T_{air}) and root zone temperature (red line, $T_{rootzone}$) in the control run at the US-Ha1 site (top), the FI-Let site (middle), and the FI-Hyy site (bottom).

Figure 4. Comparison between observed and simulated mean half-hour values of latent and sensible heat fluxes during March, April, and May (MAM, a and b) and whole year (c and d) at the US-Ha1 site with four model simulations: S01 (black, control), S02 (blue, eT_DE), S03 (red, pT) and S04 (green, eT_SE). The circle means observation values. The definition of model simulations is in Table 1.

Figure 5. Comparison between observed and simulated mean half-hour values of latent and sensible heat fluxes during May, June, and July (MJJ, a and b) and whole year (c and d) at the FI-Let site with four model simulations: S01 (black, control), S02 (blue, eT_DE), S03 (red, pT) and S04 (green, eT_SE). The circle means observation values. The definition of model simulations is in Table 1.

Figure 6. Comparison between observed and simulated mean half-hour values of latent and sensible heat fluxes during May, June, and July (MJJ, a and b) and whole year (c and d) at the FI-Hyy site with four model simulations: S01 (black, control), S02 (blue, eT_DE), S03 (red, pT) and S04 (green, eT_SE). The circle means observation values. The definition of model simulations is in Table 1.

Figure 7. Comparison between observed and simulated climatological daily averaged values of sensible (left) and latent (bottom) heat at the US-Ha1 site (a and b), the FI-Let site (c and d), and the FI-Hyy site (e and f) with four model simulations: S01 (black, control), S02 (blue, eT_DE), S03 (red, pT) and S04 (green, eT_SE). The circle means observation values. The definition of model simulations is in Table 1.

Figure 8. The difference among the simulated monthly mean sensible (left) and latent (bottom) heat at the US-Ha1 site (a and b), the FI-Let site (c and d), and the FI-Hyy site (e and f) with four model simulations: S01 (black, control), S02 (blue, eT_DE), S03 (red, pT) and S04 (green, eT_SE). The circle means observation values. The definition of model simulations is in Table 1.

Figure 9. Comparison between the observed and the simulated sensible (a, b, c, and d) and latent (e, f, g, and h) heat at the US-Ha1 site from four model simulations: S01 (control), S02 (eT_DE), S03 (pT) and S04 (eT_SE). The solid black line represented the linear regression between the simulation and the observation. The definition of model simulations is in Table 1.

Figure 10. Differences of 10 years mean seasonal latent heat (W/m^2) between FLUXNET-MTE and the control run S01 in the Northern Hemisphere in two seasons: a and b for MAM and JJA (from the left column to the right column). And differences of 10 years mean seasonal latent heat between the control run and three sensitivity simulations: S02 (c and d), S03 (e and f), and S04 (g and h) in these two seasons. The definition of model simulations is in Table 1.

Figure 11. Differences of 10 years mean seasonal latent heat (W/m^2) between FLUXNET-MTE and the control run S01 in the Northern Hemisphere in two seasons: a and b for SON and DJF (from the left column to the right column). And differences of 10 years mean seasonal latent heat between the control run and three sensitivity simulations: S02 (c and d), S03 (e and f), and S04 (g and h) in these two seasons. The definition of model simulations is in Table 1.

Figure 12. Differences of spatially averaged monthly latent heat (W/m^2) between FLUXNET-MTE and four model simulations over North America and Siberia: S01 (control), S02 (eT_DE), S03 (pT), and S04 (eT_SE). The definition of model simulations is in Table 1.

Table Captions:

Table 1. Definitions of the control simulation and sensitivity simulations.

Table 2. Model performance for simulating sensible (Qh) and latent (Qle) heat indicated by the root mean square error (RMSE) and the agreement index (d) between the model results and the observed data at three FLUXNET sites. The simulations code (S01, S02, S03, and S04) is defined in Table 1.

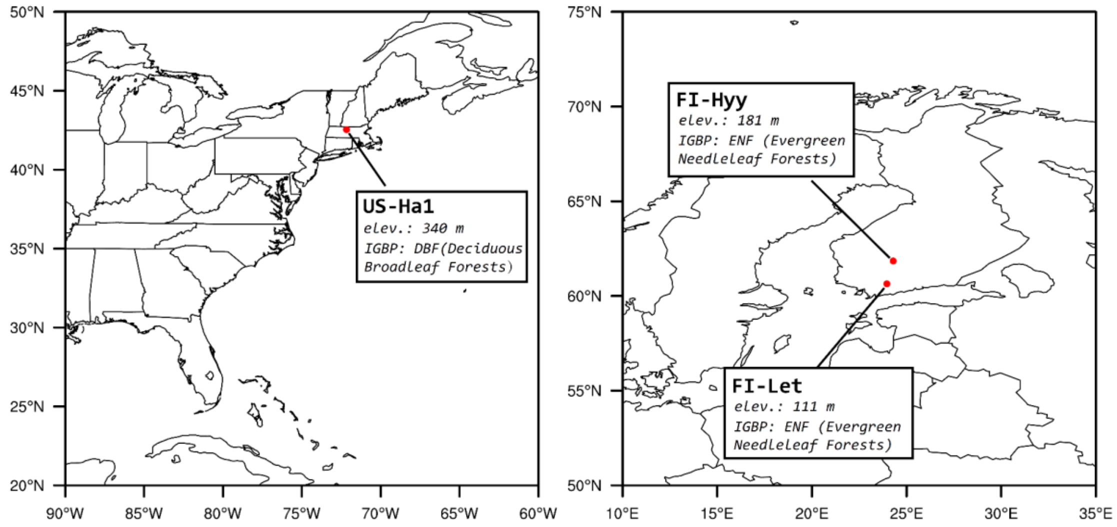

Figure 1. The location and the IGBP (International Geosphere-Biosphere Programme) type of the US-Ha1 site, the FI-Let site, and the FI-Hyy site.

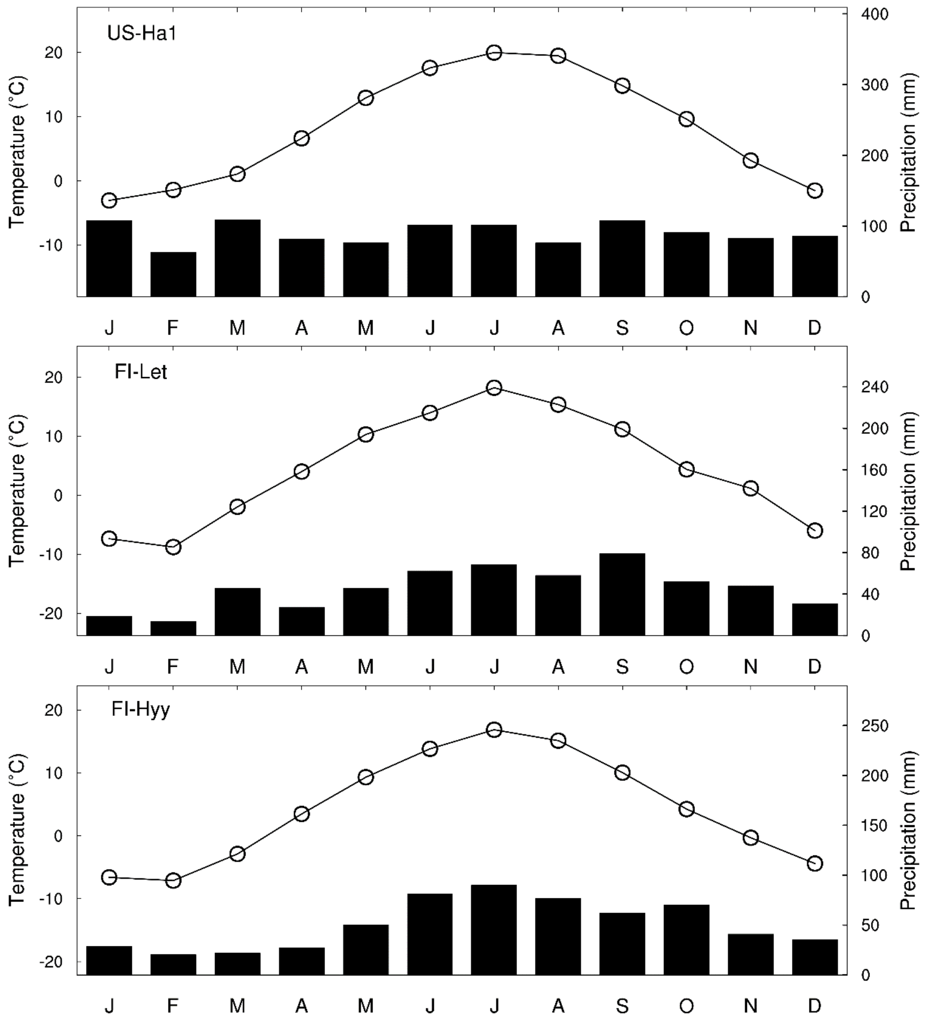

Figure 2. Observed climatological monthly averaged precipitation (bar) and temperature (line with the circle) at the US-Ha1 site (top), the FI-Let site (middle), and the FI-Hyy site (bottom).

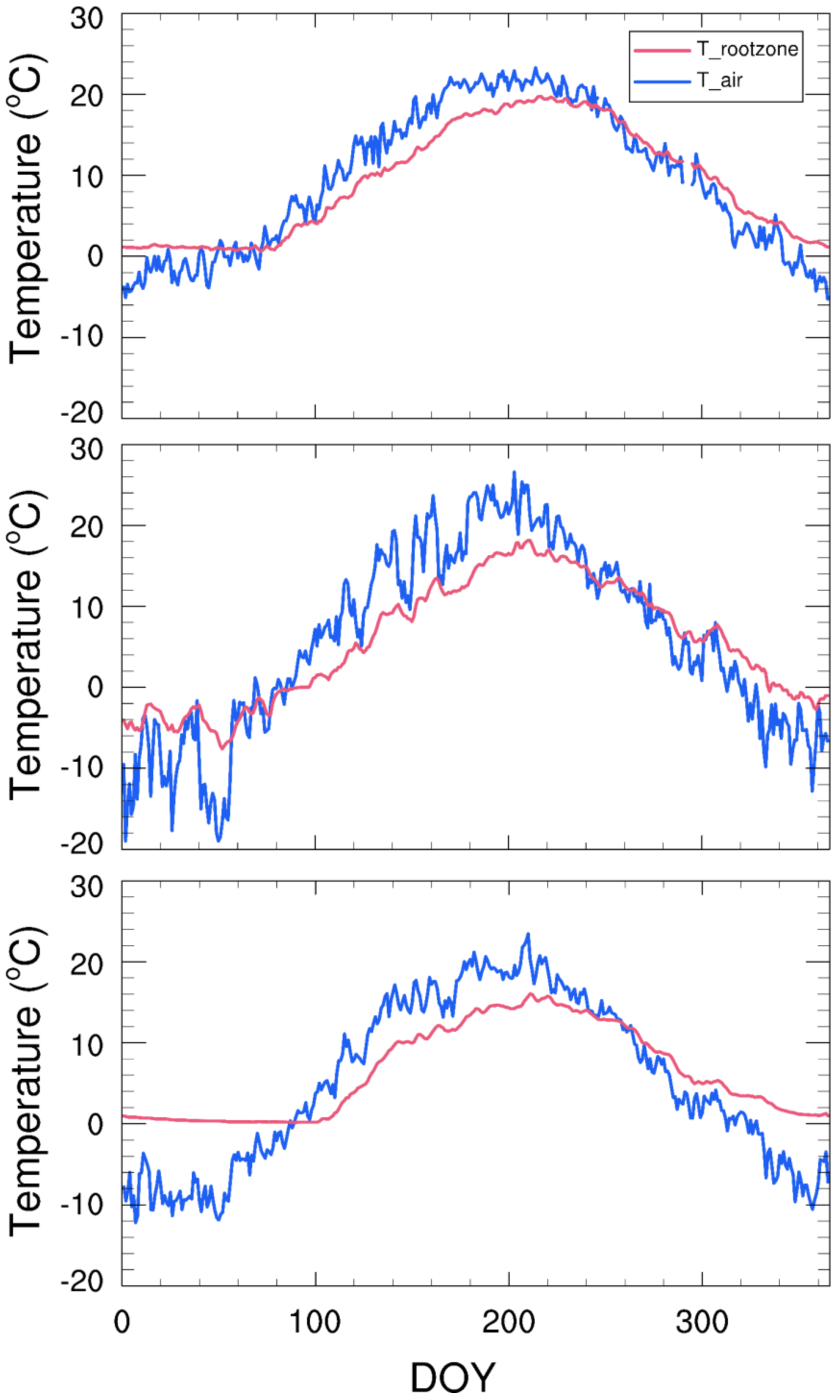

Figure 3. Simulated climatological daily averaged of air temperature (blue line, T_{air}) and root zone temperature (red line, $T_{rootzone}$) in the control run at the US-Ha1 site (top), the FI-Let site (middle), and the FI-Hyy site (bottom).

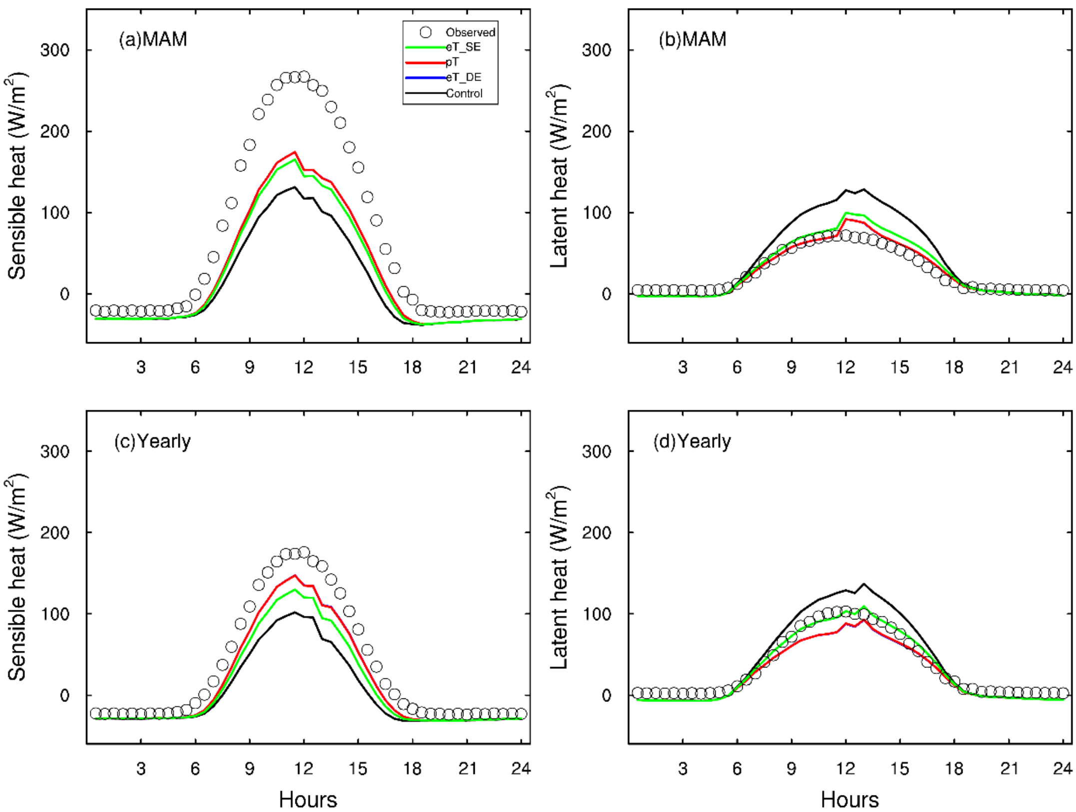

Figure 4. Comparison between observed and simulated mean half-hour values of latent and sensible heat fluxes during March, April, and May (MAM, a and b) and whole year (c and d) at the US-Ha1 site with four model simulations: S01 (black, control), S02 (blue, eT_DE), S03 (red, pT) and S04 (green, eT_SE). The circle means observation values. The definition of model simulations is in Table 1.

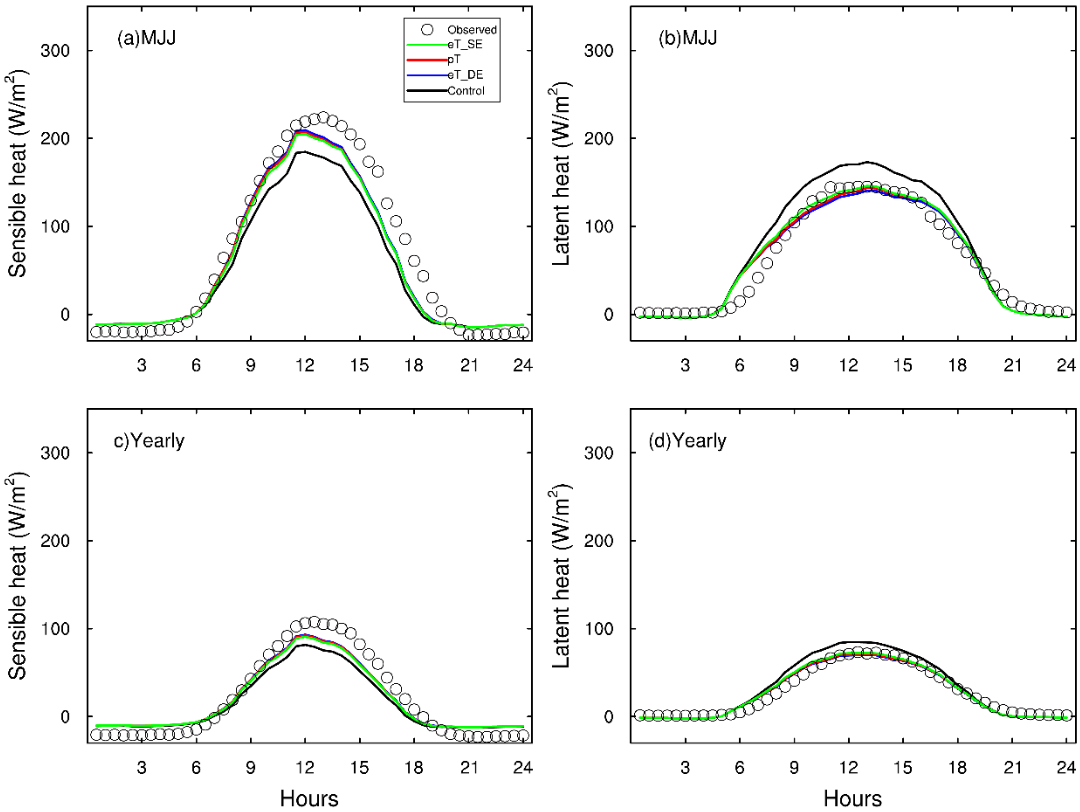

Figure 5. Comparison between observed and simulated mean half-hour values of latent and sensible heat fluxes during May, June, and July (MJJ, a and b) and whole year (c and d) at the FI-Let site with four model simulations: S01 (black, control), S02 (blue, eT_DE), S03 (red, pT) and S04 (green, eT_SE). The circle means observation values. The definition of model simulations is in Table 1.

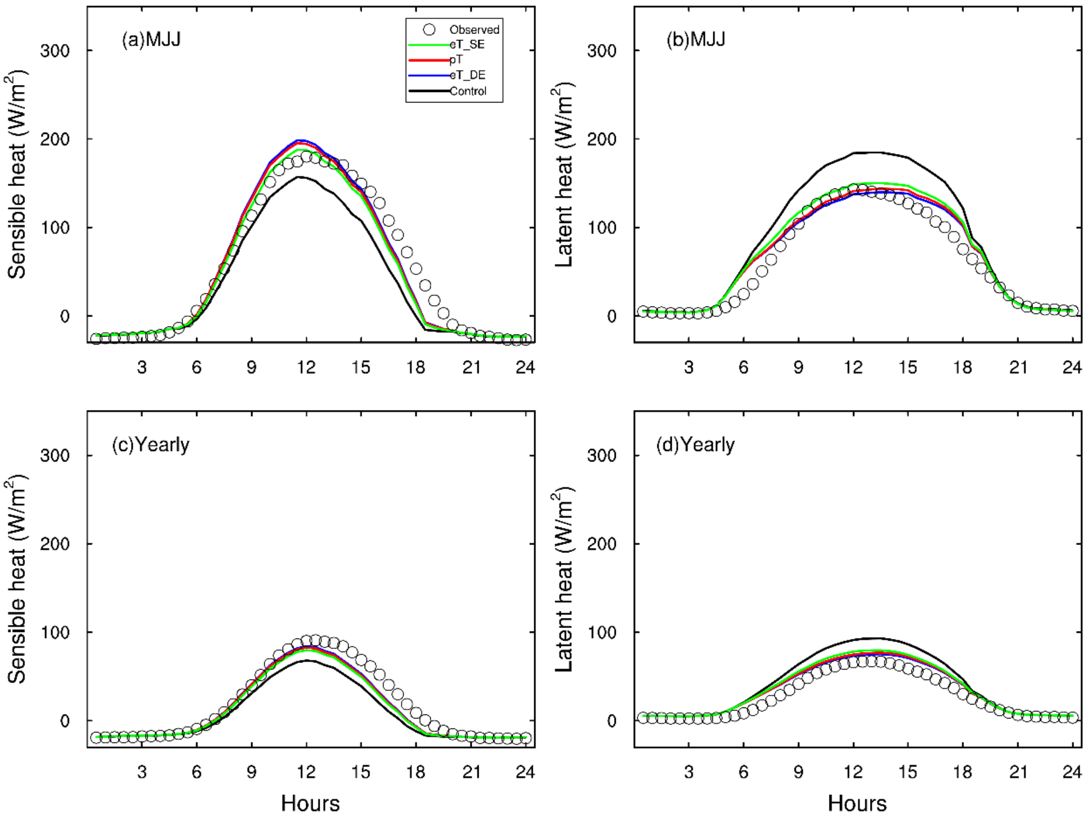

Figure 6. Comparison between observed and simulated mean half-hour values of latent and sensible heat fluxes during May, June, and July (MJJ, a and b) and whole year (c and d) at the FI-Hyy site with four model simulations: S01 (black, control), S02 (blue, eT_DE), S03 (red, pT) and S04 (green, eT_SE). The circle means observation values. The definition of model simulations is in Table 1.

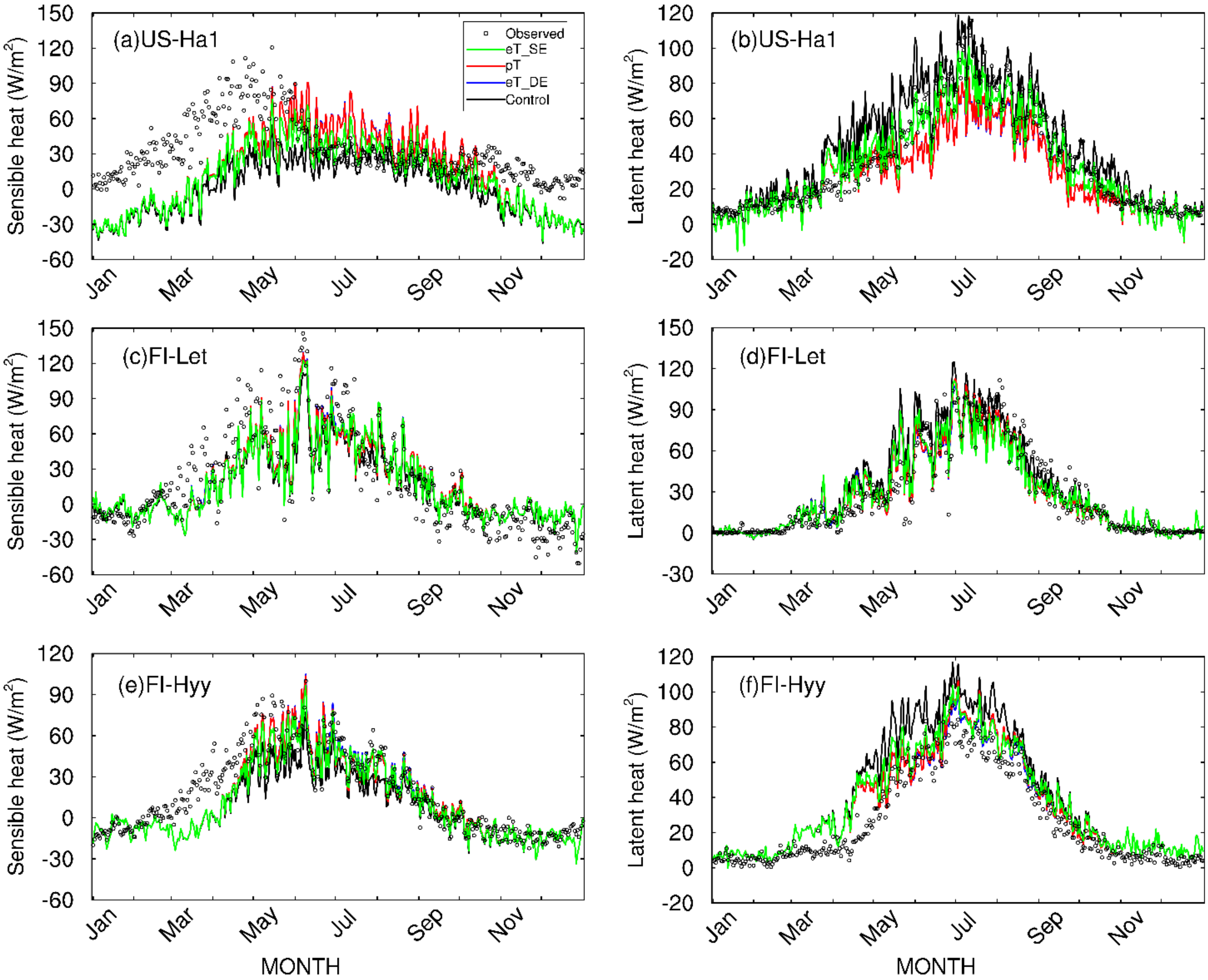

Figure 7. Comparison between observed and simulated climatological daily averaged values of sensible (left) and latent (bottom) heat at the US-Ha1 site (a and b), the FI-Let site (c and d), and the FI-Hyy site (e and f) with four model simulations: S01 (black, control), S02 (blue, eT_DE), S03 (red, pT) and S04 (green, eT_SE). The circle means observation values. The definition of model simulations is in Table 1.

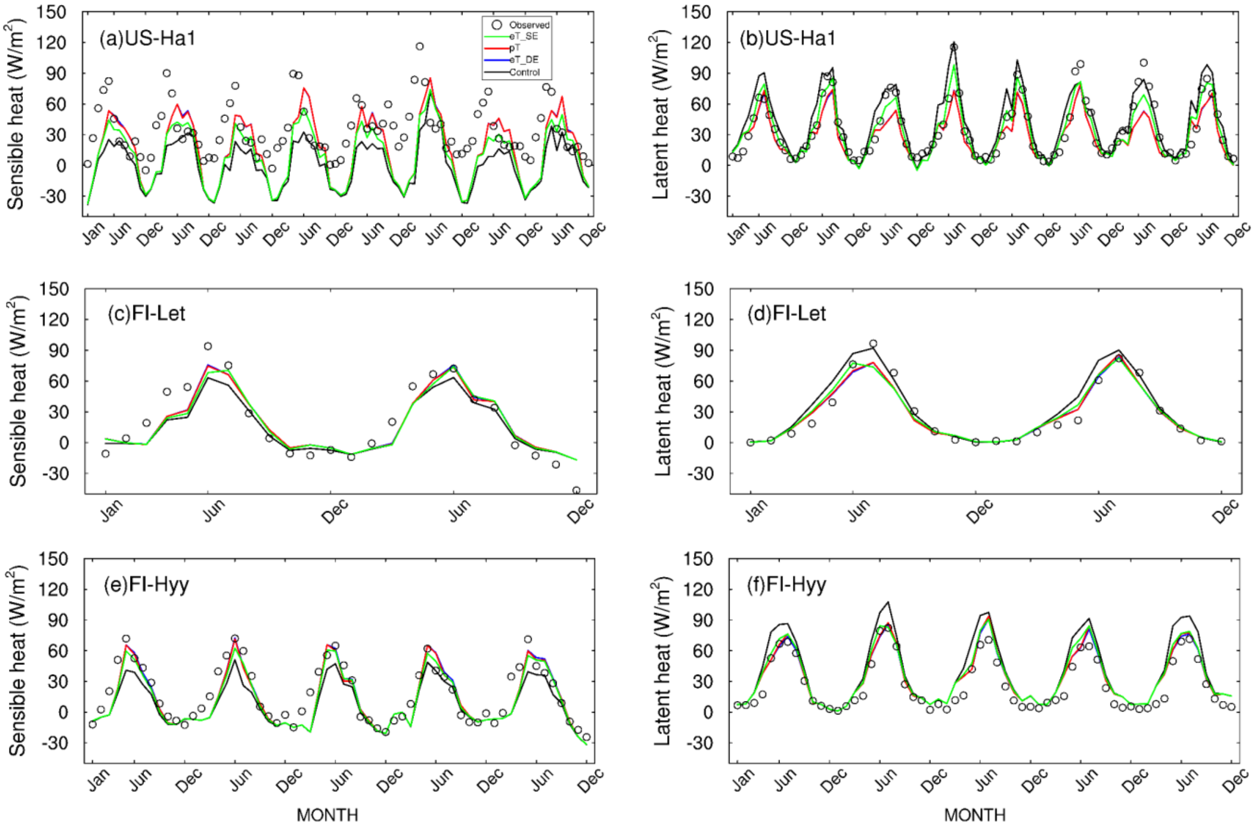

Figure 8. The difference among the simulated monthly mean sensible (left) and latent (bottom) heat at the US-Ha1 site (a and b), the FI-Let site (c and d), and the FI-Hyy site (e and f) with four model simulations: S01 (black, control), S02 (blue, eT_DE), S03 (red, pT) and S04 (green, eT_SE). The circle means observation values. The definition of model simulations is in Table 1.

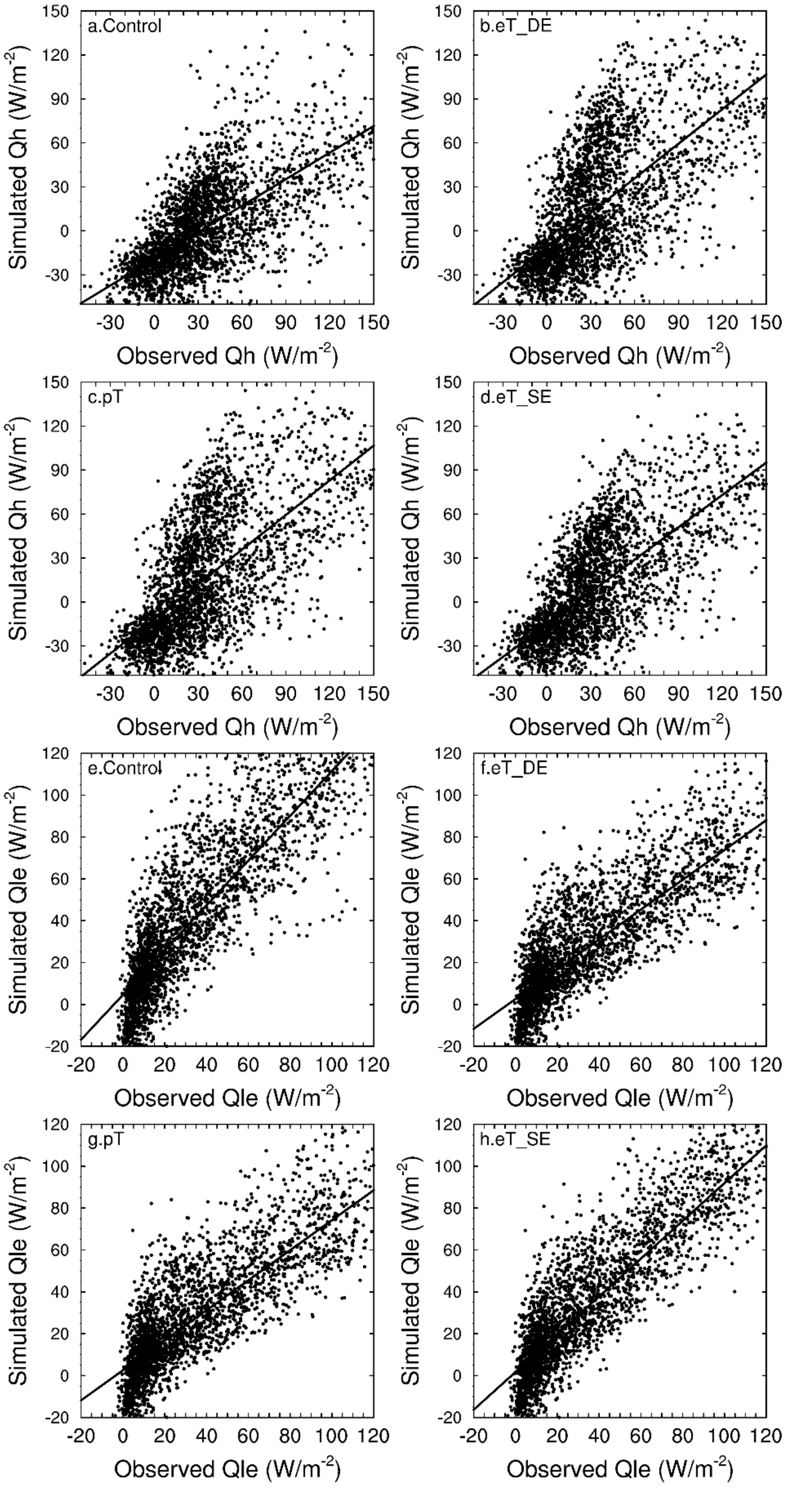

Figure 9. Comparison between the observed and the simulated sensible (a, b, c and d) and latent (e, f, g, and h) heat at the US-Ha1 site from four model simulations: S01 (control), S02 (eT_DE), S03 (pT) and S04 (eT_SE). The solid black line represented the linear regression between the simulation and the observation. The definition of model simulations is in Table 1.

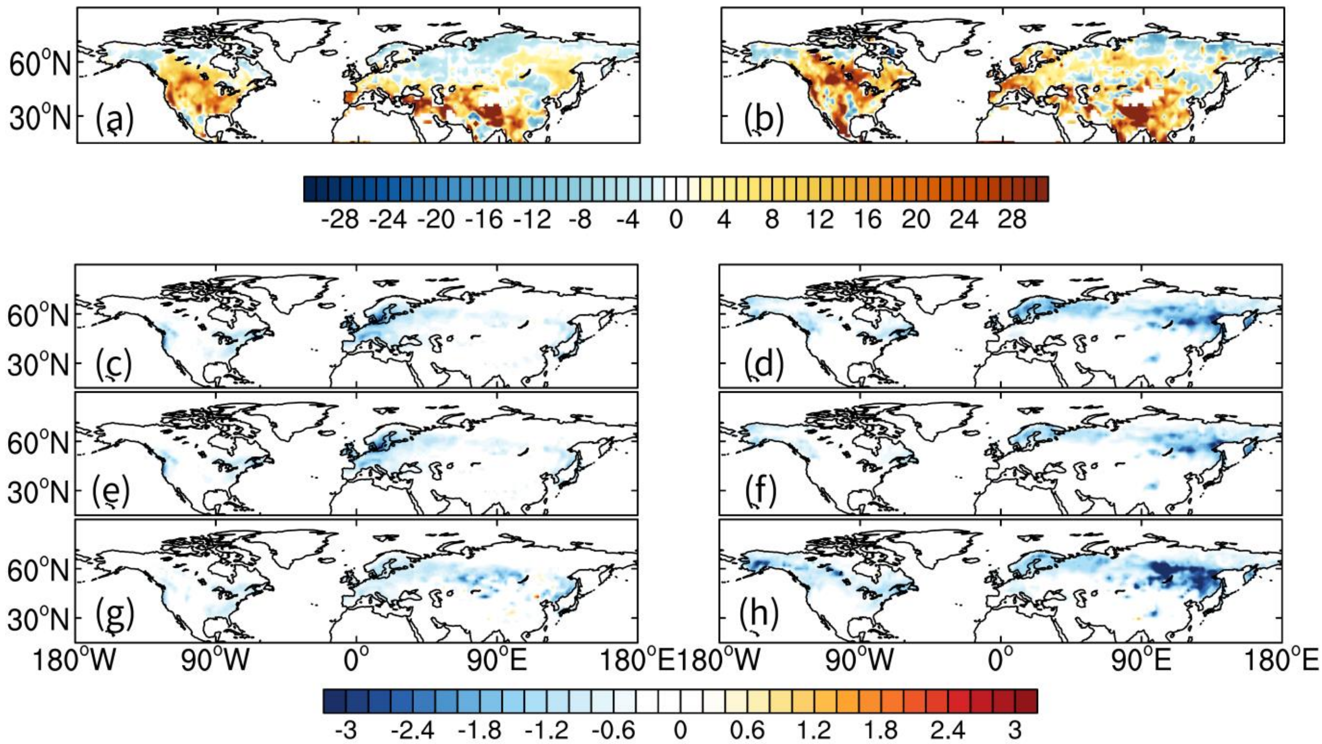

Figure 10. Differences of 10 years mean seasonal latent heat (W/m^2) between FLUXNET-MTE and the control run S01 in the Northern Hemisphere in two seasons: a and b for MAM and JJA (from the left column to the right column). And differences of 10 years mean seasonal latent heat between the control run and three sensitivity simulations: S02 (c and d), S03 (e and f), and S04 (g and h) in these two seasons. The definition of model simulations is in Table 1.

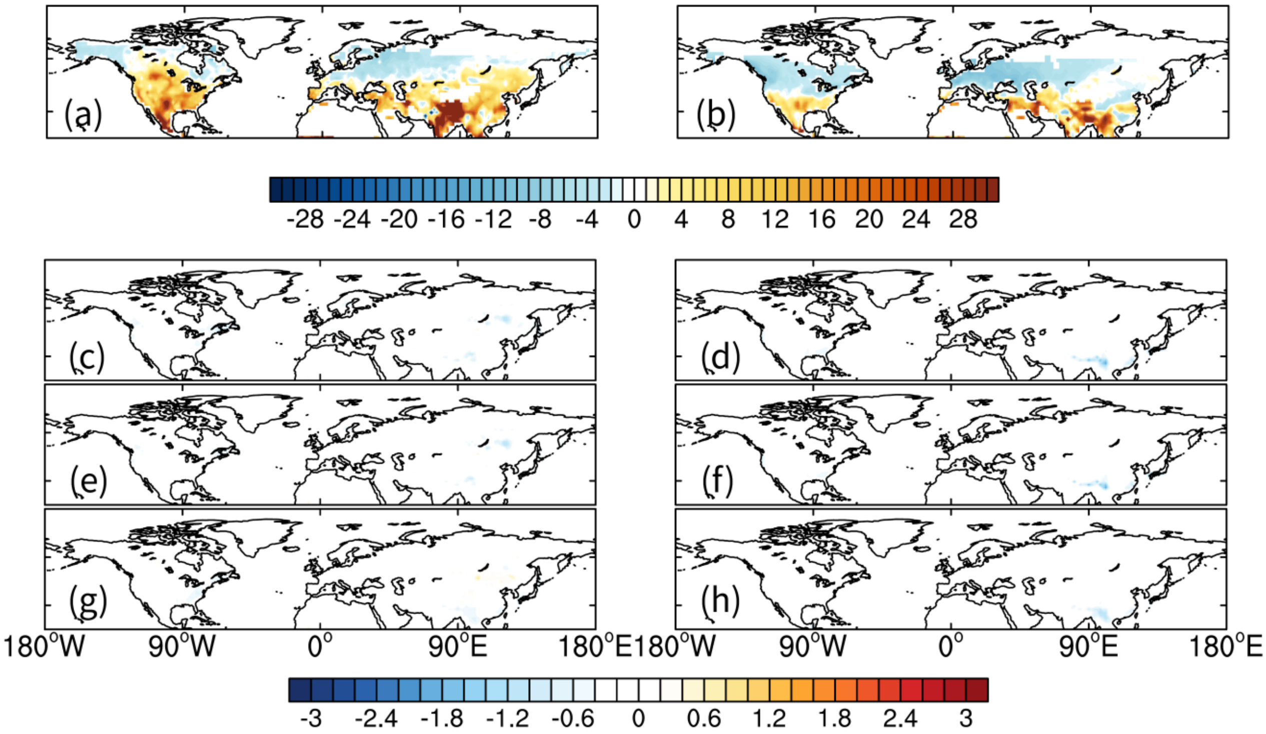

Figure 11. Differences of 10 years mean seasonal latent heat (W/m^2) between FLUXNET-MTE and the control run S01 in the Northern Hemisphere in two seasons: a and b for SON and DJF (from the left column to the right column). And differences of 10 years mean seasonal latent heat between the control run and three sensitivity simulations: S02 (c and d), S03 (e and f), and S04 (g and h) in these two seasons. The definition of model simulations is in Table 1.

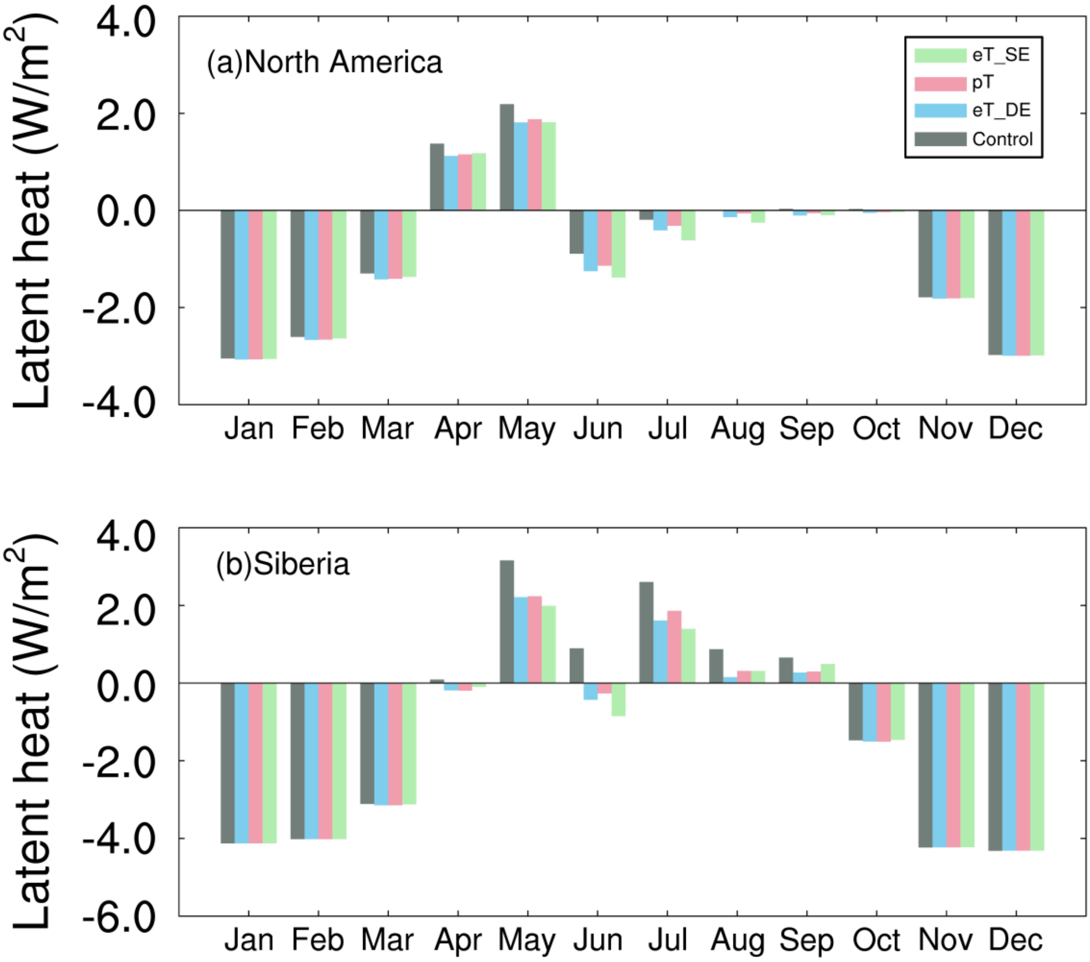

Figure 12. Differences of spatially averaged monthly latent heat (W/m^2) between FLUXNET-MTE and four model simulations over North America and Siberia: S01 (control), S02 (eT_DE), S03 (pT), and S04 (eT_SE). The definition of model simulations is in Table 1.

Table 1. Definitions of the control and sensitive simulations.

ID	Simulation	Full Name
1	S01	Default
2	S02	S01 + the double-exponential function (eT_DE)
3	S03	S01 + the polynomial function (pT)
4	S04	S01 + the single-exponential function (eT_SE)

Table 2. Model performance for simulating sensible (Qh) and latent (Qle) heat indicated by the root mean square error (RMSE) and the agreement index (d) between the model results and the observed data at three FLUXNET sites. The simulations code (S01, S02, S03, and S04) is defined in Table 1.

	Index	Variable	S01	S02	S03	S04
			US-Ha1			
MAM	d	Qh	0.82	0.89	0.89	0.88
		Qle	0.75	0.75	0.75	0.77
	RMSE	Qh	100.72	83.2	83.18	86
		Qle	56.01	45.02	44.97	46.1
Annual	d	Qh	0.83	0.88	0.88	0.88
		Qle	0.9	0.86	0.86	0.9
	RMSE	Qh	71.57	66.52	66.55	64.71
		Qle	46.75	46.93	47.17	42.48
			FI-Let			
MJJ	d	Qh	0.83	0.86	0.86	0.84
		Qle	0.84	0.86	0.86	0.84
	RMSE	Qh	33.10	30.15	30.67	31.99
		Qle	25.25	21.77	22.19	23.69
Annual	d	Qh	0.91	0.92	0.92	0.91
		Qle	0.95	0.95	0.95	0.94
	RMSE	Qh	23.60	22.92	23.12	23.61
		Qle	15.27	14.44	14.58	15.16
			FI-Hyy			
MJJ	d	Qh	0.81	0.91	0.90	0.91
		Qle	0.72	0.84	0.83	0.82
	RMSE	Qh	28.47	20.83	21.49	20.80
		Qle	28.67	17.67	18.88	19.05
Annual	d	Qh	0.87	0.92	0.92	0.92
		Qle	0.91	0.93	0.93	0.93
	RMSE	Qh	22.76	19.76	20.00	19.84
		Qle	19.92	14.53	15.02	15.30